Better DC Bus Utilization and Torque Ripple Reduction by using SVPWM for VSI fed Induction Motor Drive

K .Gopala Krishna, T. Kranthi Kumar, and P. Venugopal Rao

***Abstract*—The maximum value of the peak-phase voltage that can be obtained from a 3-Ph inverter with Sinusoidal Pulse Width Modulation (SPWM) technique is equal to $0.5V_{dc}$ It can be improved to $0.577V_{dc}$ by Space Vector Pulse Width Modulation (SVPWM). So that a better DC bus utilization compared to SPWM (by about 15.4%). With the Conventional Direct Torque Control scheme employing a Voltage Source Inverter (VSI), it is possible to control directly the stator flux linkage and the electromagnetic torque by the optimum selection of inverter switching vectors. The selection of inverter switching vector is made to restrict the flux and torque errors within the respective flux and torque hysteresis bands. However, DTC drives utilizing hysteresis comparators suffer from high torque ripple and variable switching frequency. The most common solution to this problem is to use the Space Vector Modulation. This achieves lower switching losses, better DC bus utilization, lower torque ripple, constant switching frequency. In this paper the modeling and simulation of induction motor drive employing SVM-DTC was carried out using MATLAB/SIMULINK simulation package and results are compared with Conventional DTC.**

***Index Terms*— DTC, VSI, SVM.**

I. Introduction

The name Direct Torque Control is derived from the fact that, on the basis of error between the reference and the estimated values of torque and flux, it is possible to directly control the inverter states in order to reduce the torque and flux errors with in prescribed limits. In [4], [7]-[9], different methods have been presented which allow constant switching frequency operation. In general, they require control schemes which are more complex with respect to the basic DTC scheme. With reference to current and torque ripple it has been verified that a large influence is exerted by the amplitude of flux and torque hysteresis bands, and the voltage vector selection criteria [3], [11]. It can be noted also that a given voltage vector has a different effect on the drive behavior at high and low speed. Taking these considerations into account, a good compromise has been obtained using different switching tables at high and low speed [11].

In general, the determination of the switching tables is carried out on the basis of physical considerations concerning the effects determined by radial and tangential variations of the stator flux vector on torque and flux values. Although simple, this approach leads to unexpected torque variations in some particular operating conditions. The understanding of these phenomena requires a rigorous analytical approach taking the electromagnetic behavior of the machine into account [2], [6]. A substantial reduction of current and torque ripple could be obtained using, at each cycle period, a preview technique in the calculation of the stator flux vector variation required to exactly compensate the flux and torque errors [4], [8]. In order to apply this principle, the control system should be able to generate, at each sampling period, any voltage vector (e.g., using the Space Vector Modulation technique).

The closed-loop stator flux predictive control, open-loop torque control using space-vector Modulation (SVM) implementation is shown in [5]. The SVM is a Performant open-loop vector modulation strategy [10]. This paper introduces a new direct torque and flux control based on SVM (DTC-SVM) for IM drives. It implements closed-loop control for both flux and torque in a similar manner as DTC, but the voltage is produced by an SVM unit. This way, the DTC transient performance and robustness are preserved and the steady-state torque ripple is reduced. Additionally, the switching frequency is constant and totally controllable.

II. Principle of SVM-DTC

Space Vector Modulation is one of the PWM technique in which, when the drive is excited by 3-ø balanced currents produces a voltage space vector which traces a circle with uniform velocity by sampling that rotating reference voltage space vector with high sampling frequency different switching's can be possible. It is similar to Sine-Triangle PWM in which sinusoidal frequency is proportional to rotating space vector and triangle wave frequency is proportional to sampling frequency.

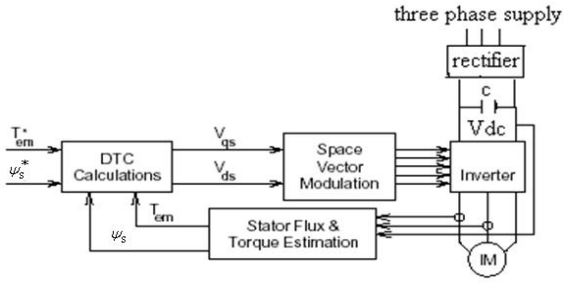

Fig. 1. Block diagram of SVM-DTC.

In the block diagram directly AC supply is not connect to Induction Motor because for majority of applications, a wide range of frequency variation is desirable. That's why 3-ø AC is connected diode rectifier which converts AC to DC, diode rectifier because it improves power factor. Rectified DC output is fed to inverter to convert it to AC. They are broadly

Manuscript received February 20, 2012; revised March 30, 2012.

K. G. Krishna is with the EEE Department at Adam's Engineering College (Accredited by NBA), Paloncha.

T. K. Kumar is with the EEE Department at Avanthi Institute of Engineering and Technology, Hyderabad.

P. V. Rao is with the Department at SR Engineering College (Autonomous), Warangal, Andhra Pradesh.

classified depending upon source feeding them: Voltage or Current source. In both these sources, the magnitude should be adjustable. The output frequency becomes independent of input supply frequency, by means of dc link. The dc link filter consists of a capacitor to keep the input voltage to the inverter a stiff DC. This is power conversion stage. The torque and flux of induction motor are estimated and they are compared with reference torque and flux, that error is modulated in SVM and fed to the inverter so that respective inverter state is switched.

In case of DC separately excited machine by construction armature and field are orthogonal and it is easily possible to control torque and flux producing components independently. Similar to that for induction machine it is required to resolve stator current into flux producing and torque producing components for independent control.

In detail 3-ø machine dynamic model is complex because the 3-ø rotor winding moves with respect to 3-ø stator winding. So by converting 3-ø machine into equivalent 2-ø machine complexity reduces. Consider a symmetrical three-phase induction machine with stationary *as-bs-cs* axes at 2π/3-angle apart, as shown in Fig. 2 Our goal is to transform the three-phase stationary reference frame *(as~bs~cs)* variables into two-phase stationary reference frame (d^s~q^s) variables and then transform these to synchronously rotating reference frame (d^e~q^e), and vice-versa.

Assume that the d^s_ q^s Axes are oriented at Θ angle, as shown in Fig .2 The voltages V_{ds}^s and V_{qs}^s can be resolved into *as~bs~cs* components and can be represented in the matrix form as

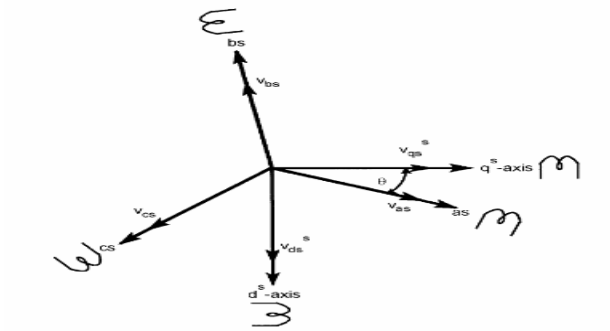

Fig. 2. Stationary frame *a~b~c* to d^s~q^s axes transformation

$$\begin{bmatrix} V_{as} \\ V_{bs} \\ V_{cs} \end{bmatrix} = \begin{bmatrix} \cos\theta & \sin\theta & 1 \\ \cos(\theta - 120^0) & \sin(\theta - 120^0) & 1 \\ \cos(\theta + 120^0) & \sin(\theta + 120^0) & 1 \end{bmatrix} \begin{bmatrix} V_{qs}^s \\ V_{ds}^s \\ V_{os}^s \end{bmatrix}$$

The corresponding inverse relation is

$$\begin{bmatrix} V_{qs}^s \\ V_{ds}^s \\ V_{os}^s \end{bmatrix} = \frac{2}{3} \begin{bmatrix} \cos\theta & \cos(\theta - 120^0) & \cos(\theta + 120^0) \\ \sin\theta & \sin(\theta - 120^0) & \sin(\theta + 120^0) \\ 0.5 & 0.5 & 0.5 \end{bmatrix} \begin{bmatrix} V_{as} \\ V_{bs} \\ V_{cs} \end{bmatrix}$$

where Voss is added as the zero sequence component, which may or may not be present.

We have considered voltage as the variable. The current and flux linkages can be transformed by similar equations. It is convenient to set Θ=0, so that the q s – axis is aligned with the as-axis. Ignoring the zero sequence components, the transformation relations can be simplified as

$$V_{as} = V_{qs}^s$$

$$. V_{bs} = -\frac{1}{2} V_{qs}^s - \frac{\sqrt{3}}{2} V_{ds}^s$$

$$. V_{cs} = -\frac{1}{2} V_{qs}^s + \frac{\sqrt{3}}{2} V_{ds}^s$$

And inversely

$$V_{qs}^s = \frac{2}{3} V_{as} - \frac{1}{3} V_{bs} - \frac{1}{3} V_{cs} = V_{as}$$

$$. V_{ds}^s = -\frac{1}{\sqrt{3}} V_{bs} + \frac{1}{\sqrt{3}} V_{cs}$$

In terms of stator resistance and flux linkages

$$V_{qs}^s = R_s i_{qs}^s + \frac{d}{dt} \psi_{qs}^s$$

$$V_{ds}^s = R_s i_{ds}^s + \frac{d}{dt} \psi_{ds}^s$$

$$0 = R_r i_{qr}^s + \frac{d}{dt} \psi_{qr}^s - \omega_r \psi_{dr}^s$$

$$0 = R_r i_{dr}^s + \frac{d}{dt} \psi_{dr}^s + \omega_r \psi_{qr}^s$$

And the torque can be written as

$$T_e = \frac{3}{2}\left(\frac{P}{2}\right) \psi_{ds}^s i_{qs}^s - \psi_{qs}^s i_{ds}^s$$

Firstly model of a three-phase voltage source inverter is presented on the basis of space vector representation is shown in Fig. 3 S1to S6 are the six power switches that shape the output, when top switch is ON taken as 1 and when bottom switch is ON taken as 0. That means for each limb two states are possible, as there are 3 limbs total 23 states are possible shown in Fig. 4

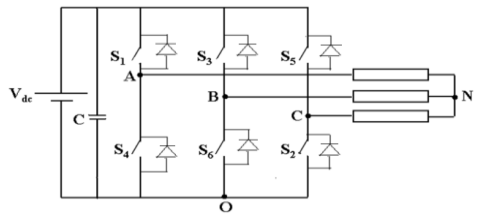

Fig. 3. Power circuit of a three-phase VSI.

As a result, six non-zero (active) vectors and two zero vectors are possible. Six non-zero vectors (V1 - V6) Shape the axes of a hexagonal as depicted in Fig 5. and feed electric power to the system. The angle between any adjacent two non-zero vectors is 60 degrees. Meanwhile, two zero vectors (V0 and V7) are at the origin and apply zero voltage to the load. The eight vectors are called the basic space vectors and are denoted by V0(000), V1(100), V2(110), V3(010), V4(011), V5(001), V6(101), V7(111). The same transformation can be applied to the desired output voltage to get the desired reference voltage vector Vref in the d-q plane.

The objective of SVPWM technique is to approximate the reference voltage vector *Vref* using the eight switching patterns. One simple method of approximation is to generate the average output of the inverter in a small period, T to be the

same as that of *Vref* in the same period.

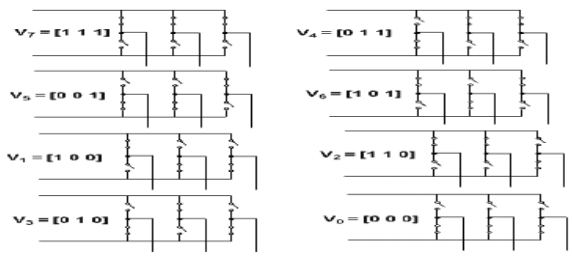

Fig. 4. Eight inverter voltages vectors (V_0 to V_7).

Therefore, space vector PWM can be implemented by the following steps:

Step 1: Determination of *Vd. Vq, Vref* and angle (α)

Step 2: Determination of time duration T1, T2, T0

Step 3: Determination of the switching time of each switch (S1 to S6)

Step 1: Determination of Vd, Vq, Vref, and angle (α)

From Fig. 5 we can write

$$V_d = V_{an} - V_{bn} \cdot \cos 60 - V_{cn} \cdot \cos 60$$
$$= V_{an} - \frac{1}{2} V_{bn} - \frac{1}{2} V_{cn}$$
$$V_q = 0 + V_{bn} \cdot \cos 30 - V_{cn} \cdot \cos 30$$

Step 2: Determination of time duration T1, T2, T0 From Fig. 5 The switching time duration can be calculated as follows:

Switching time duration at Sector 1 can be realized by V1 and V2 vectors and one of two null vectors V0 or V7.In other words, V1 state is active for time T1, V2 is active for T2, and one of null vectors (V or V7) is active for T0.Because the vectors V1 and V2 are constant and V0 or V7 is 0, We can equate the Volt time of reference vector to the Space Vector as, (here f=fundamental frequency)

$$\therefore \alpha = \tan^{-1}\left(\frac{V_q}{V_d}\right) = \omega t = 2\pi f t$$
$$\therefore T_z \cdot \overline{V}_{ref} = (T_1.\overline{V}_1 + T_2.\overline{V}_2)$$
$$\Rightarrow T_z \cdot \left|\overline{V}_{ref}\right| \cdot \begin{bmatrix} \cos\alpha \\ \sin\alpha \end{bmatrix} = T_1 \cdot \frac{2}{3}.V_{dc} \cdot \begin{bmatrix} 1 \\ 0 \end{bmatrix} + T_2 \cdot \frac{2}{3} \cdot V_{dc} \cdot \begin{bmatrix} \cos(\pi/3) \\ \sin(\pi/3) \end{bmatrix}$$

(where, $0 \le \alpha \le 60°$)

$$\therefore T_1 = T_z \cdot a \cdot \frac{\sin(\pi/3 - \alpha)}{\sin(\pi/3)}$$
$$\therefore T_2 = T_z \cdot a \cdot \frac{\sin(\alpha)}{\sin(\pi/3)}$$
$$\therefore T_0 = T_z - (T_1 + T_2) \qquad \left(where \;\; T_z = \frac{1}{f_z} \;\; and \;\; a = \frac{\left|\overline{V}_{ref}\right|}{\frac{2}{3} V_{dc}} \right)$$
$$\left(where \;\; T_z = \frac{1}{f_z} \;\; and \;\; a = \frac{\left|\overline{V}_{ref}\right|}{\frac{2}{3} V_{dc}} \right) \quad (1)$$

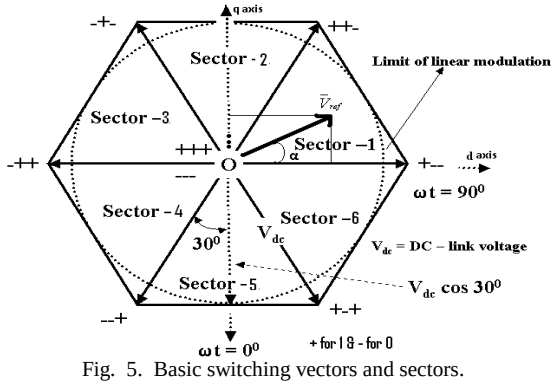

Fig. 5. Basic switching vectors and sectors.

Step 3: Determination of the switching time of each switch (S1 to S6)

The switching time for each switch is tabulate in Table I. The waveform considered in Fig. 6 is the switching pulse of the upper switch and mirror image represent the pulse of lower switch in sector 1 similarly we can realize in other sectors also.

TABLE I: SWITCHING TIME TABLE AT EACH SECTOR

Sector	Upper Switches (S_1,S_3,S_5)	Lower Switches (S_4,S_6,S_2)
1	$S_1=T_1+T_2+T_0/2$ $S_3=T_2+T_0/2$ $S_5=T_0/2$	$S_4=T_0/2$ $S_6=T_1+T_0/2$ $S_2=T_1+T_2+T_0/2$
2	$S_1=T_1+T_0/2$ $S_3=T_1+T_2+T_0/2$ $S_5=T_0/2$	$S_4=T_2+T_0/2$ $S_6=T_0/2$ $S_2=T_1+T_2+T_0/2$
3	$S_1=T_0/2$ $S_5=T_2+T_0/2$ $S_3=T_1+T_2+T_0/2$	$S_4=T_1+T_2+T_0/2$ $S_6=T_0/2$ $S_2=T_1+T_0/2$
4	$S_1=T_0/2$ $S_3=T_1+T_0/2$ $S_5=T_1+T_2+T_0/2$	$S_4=T_1+T_2+T_0/2$ $S_2=T_0/2$ $S_6=T_2+T_0/2$
5	$S_3=T_0/2$ $S_1=T_2+T_0/2$ $S_5=T_1+T_2+T_0/2$	$S_6=T_1+T_2+T_0/2$ $S_2=T_0/2$ $S_4=T_1+T_0/2$
6	$S_3=T_0/2$ $S_5=T_1+T_0/2$ $S_1=T_1+T_2+T_0/2$	$S_6=T_1+T_2+T_0/2$ $S_4=T_0/2$ $S_2=T_2+T_0/2$

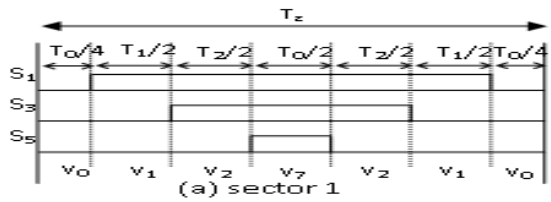

Fig. 6. SVPWM switching patterns of upper switch sector 1.

III. DC BUS UTILISATION BY SVPWM

The principal advantage of the SVPWM over SPWM is that it enhances the DC bus utilization by about 15%. It is instructive to evaluate the sample-averaged pole voltage of a phase, V_{AO} for instance, to understand this fact.

In eqn.1, $|V_{sr}|$ denotes the amplitude of the reference vector and 'α' represents the position of the reference vector with respect to the beginning of the sector in which the tip of the reference vector is situated.

From Fig. 5 During $0^0 \le \omega t \le 30^0$ the following are equations (2), (3), (4)

$$V_{AO,avg} = \frac{V_{dc}/2}{T_s}\left(-\frac{T_0}{2} - T_1 + T_2 + \frac{T_0}{2}\right) \quad (2)$$

$$V_{BO,avg} = \frac{V_{dc}/2}{T_s}\left(-\frac{T_0}{2} - T_1 - T_2 + \frac{T_0}{2}\right) \quad (3)$$

$$V_{CO,avg} = \frac{V_{dc}/2}{T_s}\left(-\frac{T_0}{2} + T_1 + T_2 + \frac{T_0}{2}\right) \quad (4)$$

During $30^0 \le \omega t \le 90^0$ the following are equations (5), (6), (7)

$$V_{AO,avg} = \frac{V_{dc}/2}{T_s}\left(-\frac{T_0}{2} + T_1 + T_2 + \frac{T_0}{2}\right) \quad (5)$$

$$V_{BO,avg} = \frac{V_{dc}/2}{T_s}\left(-\frac{T_0}{2} - T_1 - T_2 + \frac{T_0}{2}\right) \quad (6)$$

$$V_{CO,avg} = \frac{V_{dc}/2}{T_s}\left(-\frac{T_0}{2} + T_1 - T_2 + \frac{T_0}{2}\right) \quad (7)$$

Substituting eqn.1 in eqn. 2 one obtains:

$$V_{AO,avg} = \frac{V_{dc}/2}{T_s} * \frac{|V_{sr}|}{V_{dc}} * \frac{T_s}{\sin 60^0}\left(-\sin(60^0 - \alpha) + \sin\alpha\right) \quad (8)$$

Noting that $\omega t = \alpha - 30^0$, when $\omega t \le 30^0$ and simplifying,

$$V_{AO,avg} = |Vsr|\, Sin\omega t \quad (9)$$

Substituting eqn.1 in eqn. 5 one obtains equation (10) below:

$$V_{AO,avg} = \frac{V_{dc}/2}{T_s} * \frac{|V_{sr}|}{V_{dc}} * \frac{T_s}{\sin 60^0}\left(\sin(60^0 - \alpha) + \sin\alpha\right) \quad (10)$$

Noting that $\omega t = \alpha + 30^0$, when $30^0 \le \omega t \le 90^0$ and simplifying,

$$V_{AO,avg} = \frac{|Vsr|}{\sqrt{3}} Sin(\omega t + 30^0) \quad (11)$$

The average pole voltage variation is plotted in Fig. 7 The waveform of the average pole voltage consists of a fundamental component and components of triplen order.

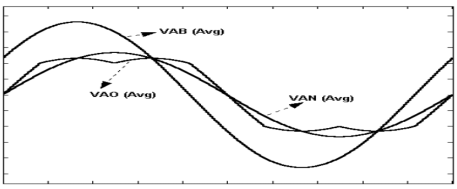

Fig. 7. Waveforms of averaged pole voltage, phase voltage and line-line voltage

The waveform of the averaged line-line voltage is sinusoidal as the triplen voltage components of the pole voltages cancel out each other, being cophasal. The averaged phase voltage also remains sinusoidal with a peak value, which is $1/\sqrt{3}$ times that of the peak value of the line-line voltage. The peak value of the A-phase voltage, while the inverter is operated in the range of linear modulation is given by:

$$V_{ph,peak} = (2/3) * |V_{sr}| \quad (12)$$

Maximum magnitude of the reference voltage space vector corresponds to the radius of the biggest circle that can be inscribed in the hexagon as shown in Fig. 5 and is equal to, $\sqrt{3}/2V_{dc}$ where V_{dc} is the input DC voltage. Thus, the maximum value of the peak-phase voltage is given by

$$V_{ph,peak,\max} = \frac{2}{3} * \frac{\sqrt{3}}{2} * V_{dc} = \frac{V_{dc}}{\sqrt{3}} = 0.577 * V_{dc} \quad (13)$$

It is known that the maximum value of the peak-phase voltage that can be obtained from a 3-Ph inverter with Sinusoidal Pulse Width Modulation (SPWM) technique is equal to $0.5V_{dc}$ It is therefore evident that SVPWM achieves a better DC bus utilization compared to SPWM (by about 15.4%).

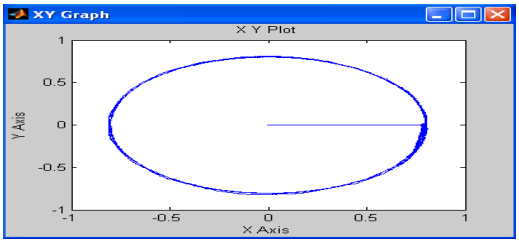

Fig. 8. d-q stator flux with SVM-DTC.

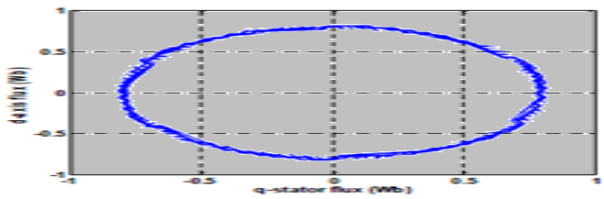

Fig. 9. d-q stator flux with a conventional DTC.

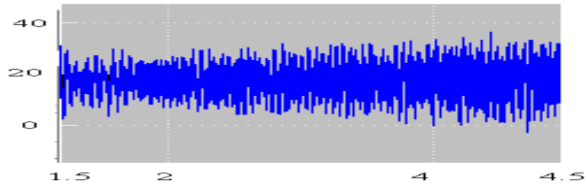

Fig. 10. Output torque with SVM-DTC.

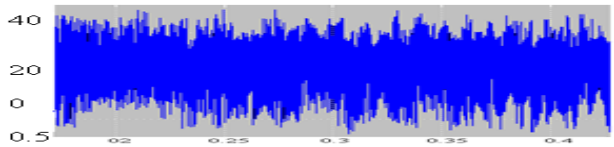

Fig. 11. Output torque with conventional DTC.

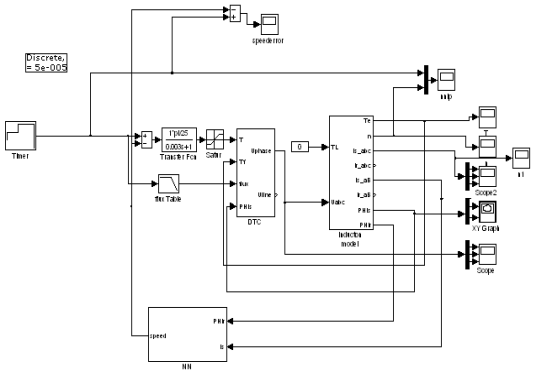

Fig. 12. SVM-DTC Simulink model.

Simulation was carried out on a 3-ø induction motor having Stator resistance: 2.7Ω, Stator inductance: 0.3562H, Rotor resistance: 2.23 Ω, Rotor inductance: 0.3562H, Mutual inductance: 0.3425H, Frictional coefficient: 0.00825, Number of poles: 2. Switching frequency: 5KHz. Fig. 12 shows Simulink model of SVM-DTC. Fig. 8-11 shows the results of conventional DTC, SVM-DTC.

IV. Conclusion

From the Simulation results it is clearly observed that DTC drive utilizing hysteresis comparator (Conventional-DTC) suffers from high torque ripple and variable switching frequency. By using constant switching frequency technique (SVM-DTC) torque ripple is significantly improved. Thus it is possible to conclude that SVM-DTC can offer high performance characteristics than conventional-DTC.

References

[1] A. Mir, D. S. Zinger, and M. E. Elbuluk, "Fuzzy implementation of direct self control of induction motors," *IEEE Trans. Ind. Applicat*, vol. 30.

[2] A. Tani, D. Casadei, and G. Serra, "Analytical investigation of Torque and flux ripple in DTC schemes for induction motors," in *Proc. IECON'97*, New Orleans, LA.

[3] A. Tani, D. Casadei, G. Grandi, and G. Serra, "Effects of flux and torque hysteresis band amplitude in direct torque control of induction machines," in *Proc. IECON'94*, Bologna, Italy, pp. 5–9, 1994.

[4] A. Tani, D. Casadei, and G. Serra, "Stator flux vector control for high performance induction motor drives using space vector modulation," *Electromotion*, vol. 2, no. 2.

[5] A. Tani, D. Casadei, and G. Sera, "Stator flux vector control For high performance induction motor drives using space vector modulation," in *Proc. OPTIM'96*.

[6] B. de Fornel, E. V. Westerholt, I. El Hassan, and X. Roboam, "Torque dynamic behavior of induction machine DTC in 4 Quadrant operation," in *Proc. ISIE'97*, Guimaraes, Portugal.

[7] C. Lochot, P. Maussion, and X. Roboam, "A new direct torque control strategy for an induction motor with constant switching frequency operation," in *Proc. EPE'95*, Spain.

[8] "Constant frequency operation of a DTC induction motor drive for electric vehicle," in *Proc. ICEM'96*, vol. III, Vigo, Spain, Sept.

[9] F. Profumo, L. M. Tolbert, M. Pastorelli, and T. G. Habetler, "Direct torque control of induction machines using space vector modulation," *IEEE Trans. Ind. Applicat.*, vol. 28, Sept./Oct.'92.

[10] J. K. Pedersen and P. Thoegersen, "Stator flux oriented asynchronous vector modulation for AC-drives," in *Proc. IEEE PESC'90*.

[11] "Switching strategies in direct torque control of induction machines," in *Proc. ICEM'94*, Paris, France, Sept.

[12] K. G. Krishna and P. V. Rao, "Space Vector Pulse Width Modulation for Two Level Inverter feeding Induction Motor" in Proc. NCEEE'10, 2010.

[13] K. G. Krishna and P. V. Rao, "Torque ripple reduction by using Space Vector Pulse Width Modulation for VSI fed Induction Motor drive" in Proc. NPEC'10, 2010.

K. Gopala Krishna working as Assistant Professor in EEE Department at Adam's Engineering College Accredited by NBA), Paloncha. He completed his Post Graduation in Power Electronics from SR Engineering College (*Autonomous*), Warangal, Andhra Pradesh. And he completed Graduation in EEE from Adam's Engineering College (Accredited by NBA), Paloncha. His papers published in International Journals, National and International Conferences Proceedings. And he is life member of Indian Society for Technical Education.

T. Kranthi Kumar working as Assistant Professor in EEE Department at Avanthi Institute of Engineering and Technology, Hyderabad. He completed Graduation in EEE from Adam's Engineering College (Accredited by NBA), Paloncha. His papers published in International Journals, National and International Conferences Proceedings. And he is life member of Indian Society for Technical Education.

P. Venugopal Rao working as Professor and Head of the Department at SR Engineering College (*Autonomous*), Warangal, Andhra Pradesh. Many of his papers published in International Journals, National and International Conferences Proceedings. And he is life member of Indian Society for Technical Education. His Research areas include Wavelets and their application to Power Systems, Power and Industrial Drives etc.